

Anchored Retaining Walls in Granite Residual Soils II. A Method for Preliminary Design

N. Raposo, A.T. Gomes, M.M. Fernandes

Abstract. In a companion paper, an extensive parametric study regarding anchored retaining structures was presented, contributing to better understand the behaviour and most relevant parameters regarding their design. Based on those results, a novel and simple methodology for preliminary design is presented, providing an alternative procedure for preliminary design and implementation of the observational method. The methodology consists on the following four steps: definition of the properties of the excavation to be analysed – target excavation; selection, among all the excavations simulated in the parametric study, of the reference excavation, that acts as a starting point; calculation of all the correction factors; prediction of the bending moments and movements of the target excavation. The paper finishes with the application of the proposed methodology to several examples of increasing complexity, allowing to show how the method is applied and simultaneously demonstrating its potential for practical purposes.

Keywords: forces and displacements, residual soil, anchored wall, preliminary design.

1. Introduction

In a companion paper (Raposo et al., 2017) it was presented a parametric study analyzing a large number of excavations supported by anchored walls. The geotechnical conditions assumed correspond to granite residual soils.

Based on that parametric study, this paper presents a simple numerical method that permits to estimate, with a reasonable approximation, the relevant results for a preliminary design of anchored walls used to support deep excavations in similar geotechnical conditions.

The task to be accomplished consists in obtaining a quick estimate for the maximum bending moment in the wall and the maximum horizontal displacement of the wall just on the basis of the parametric study results, that is, without analyzing the excavation using the finite element method or other numerical tool.

A strategy similar to the one followed by Mana (1978) and (Mana & Clough, 1981) was adopted, with innovations regarding the mathematical process.

As the maximum bending moment and the maximum horizontal displacement of the wall were calculated as function of eight variables, for which typically six different values were considered, a conventional interpolation procedure would have required more than one million analyses ($6^8 = 1679616$).

Having this in mind, an alternative method was developed, resulting in a large reduction of the total number of calculations to 158 (Raposo, 2007).

The paper presents some examples of gradually increasing complexity, highlighting the application of the de-

veloped approach. The results seem to prove the utility of the method but show, as well, its limitations.

2. Procedure for Applying the Proposed Method

2.1. General description

The proposed methodology was devised for preliminary design purposes and thus it is necessarily simple. The main aspiration is the possibility of obtaining the maximum bending moments and wall displacements, parameters that assume vital importance in the design of retaining structures. The idea is that of obtaining these parameters from accumulated experience in similar calculations. The method may easily be adapted to different geotechnical scenarios and geometrical conditions, which constitutes a great advantage. It has also the significant benefit of being an alternative procedure with respect to finite element calculations, providing an additional check for designers.

In simple terms, the method consists in the following four steps:

- A. Definition of the *target excavation*. The *target excavation* is the excavation whose preliminary design is required and should be characterized by the following parameters: excavation depth; bedrock depth; strength, stiffness and initial stress state of the ground; stiffness and prestress of the retaining structure. Table 1 presents the definition of the parameters and the variation range adopted in the parametric study (presented in the companion paper).
- B. Selection of the *reference excavation*. The *reference excavation* is to be chosen among the various excava-

Nuno Raposo, Ph.D., Adjunct Professor, Department of Civil Engineering, Viseu Polytechnic Institute, Viseu, Portugal. e-mail: nraposo@ipv.pt.
António Topa Gomes, Ph.D., Assistant Professor, Faculty of Engineering (FEUP), University of Porto, Porto, Portugal. e-mail: atgomes@fe.up.pt.
Manuel de Matos Fernandes, Ph.D., Full Professor, Faculty of Engineering (FEUP), University of Porto, Porto, Portugal. e-mail: mfern@fe.up.pt.
Submitted on March 4, 2017; Final Acceptance on September 1, 2017; Discussion open until April 30, 2018.
DOI: 10.28927/SR.403243

tions previously calculated and should be as similar as possible to the *target excavation*, having in mind the ground and retaining wall characteristics. The concept of close similarity depends on the fact that different parameters have different impact on the results. The *reference excavation* may be one of the four *base excavations* whose characteristics are shown in Table 2, with results summarized in Table 3, or any other excavation previously calculated.

Table 1 - Parameters and variation range used to characterize the excavations.

Parameter	Symbol	Variation range
Excavation depth (m)	h	10 to 25
Support system stiffness ⁽¹⁾	ρ_s	40 to 1600
Prestressing index ⁽²⁾	ξ	0.1 to 0.3
Bedrock depth	D/h	1.2 to 2.0
Soil stiffness (MPa)	E_{s0}	15 to 60
Effective friction angle (°)	ϕ'	30 to 40
Effective cohesion (kPa)	c'	0 to 30
Coefficient of earth pressure at rest	K_0	0.4 to 0.6

⁽¹⁾The stiffness of the support system is calculated by the expression:

$$\rho_s = \frac{EI}{h_M^4 \gamma} \quad (1)$$

where EI represents the wall bending stiffness, h_M is the maximum vertical spacing between consecutive supports and γ the unit weight of soil. Taking as an example a wall made of concrete piles ($E = 30$ GPa) with a diameter of 0.60 m and 1.20 m separation between axes, with a maximum vertical spacing between consecutive supports of 3 m, in a soil with a unit weight of 20 kN/m³, the stiffness of the support system would be:

$$\rho_s = \frac{EI}{h_M^4 \gamma} = \frac{30 \times 10^6 \times \pi \times \left(\frac{0.60^4}{64}\right) / 1.2}{3^4 \times 20} = 100 \quad (2)$$

⁽²⁾The prestressing index (ξ) measures, in a dimensionless form, the horizontal force applied to the wall by the grid of anchors. The prestress force to be applied to each anchor, F_a , is defined by the equation:

$$F_a = \frac{\xi \gamma h h_a l_a}{\cos \alpha} \quad (3)$$

where h represents the maximum excavation depth, h_a and l_a are the average height and width of influence of each anchor, respectively, and α the tilt angle of the anchors. Taking as an example an excavation with a prestressing index of 0.15, executed in a soil with a unit weight of 20 kN/m³, down to 15 m depth, supported by ground anchors with a tilt angle of 30 degrees, spaced 3.0 m horizontally and 2.5 m vertically, the prestress force to be applied to each anchor should be:

$$F_a = \frac{\xi \gamma h h_a l_a}{\cos \alpha} = \frac{0.15 \times 20 \times 15 \times 3 \times 2.5}{\cos 30} = 390 \text{ kN} \quad (4)$$

Table 2 - Parametric analysis – *base excavation* properties.

Excavation	h (m)	ρ_s	ξ	D/h	E_{s0} (MPa)	ϕ' (°)	c' (kPa)	K_0
#A00	15	100	0.15	1.6	22.5	33	12	0.40
#B00	15	100	0.15	1.6	37.5	37	21	0.60
#C00	25	350	0.20	1.2	22.5	33	12	0.40
#D00	25	350	0.20	1.2	37.5	37	21	0.60

Table 3 - Parametric analysis – results of the *base excavations*.

Excavation	M_{\max} (kNm/m)	δh_{wall} (mm)	$\delta h_{\text{surface}}$ (mm)	$\delta v_{\text{surface}}$ (mm)	$PS_{\max}^{(1)}$ (kN/m)
#A00	193	30.4	14.2	13.1	153
#B00	132	19.4	9.9	5.1	146
#C00	685	46.0	24.2	24.0	332
#D00	437	36.0	21.0	14.0	325

⁽¹⁾ PS_{\max} is the maximum axial force in the anchors divided by the horizontal influence distance, l_a , of each anchor.

- C. Calculation of the correction factors. For each of the base variables, the factors that allow scaling the results of the *reference excavation* must be calculated. This task is accomplished using the influence curves defined in Table 4 and Table 5.
- D. Multiplication of the correction factors by the results obtained in the *reference excavation*. With this operation the predictions for the maximum bending moment and maximum horizontal displacement of the wall are obtained.

2.2. Prediction of the bending moments

The maximum bending moment can be predicted through the following expression:

$$M_{\max} = M_{ref} \times cm_h \times cm_D \times cm_{\xi} \times cm_{\rho_s} \times cm_{E_{s0}} \times cm_{\phi} \times cm_c \times cm_{K_0} \quad (5)$$

which is the maximum bending moment in the *reference excavation* multiplied by the correction factors for the several parameters involved in the problem.

The correction factors for the bending moments are obtained by dividing the influence factors for the *target excavation* by the respective influence factors for the *reference excavation*, according to the equation:

$$cm_i = \frac{\alpha_i(\text{target excavation})}{\alpha_i(\text{reference excavation})} \quad (6)$$

where variable i represents a generic parameter and α_i is the influence factor for the bending moment relative to variable i . As referred in the companion paper, α_i corresponds to the value of the function that best defines the average influence

Table 4 - Influence factors for the maximum bending moments of the wall.

Influence factor	Equation	Influence factor range	Impact grade
α_{ρ_s}	$0.04424\rho_s^{0.5318}$	0.286 to 2.405	A (8.41)
α_h	$0.07089h^{0.9723}$	0.562 to 1.886	A (3.36)
$\alpha_{E_{50}}$	$0.5188E_{50}^{-0.4814}$	0.678 to 1.468	B (2.17)
α_s	$0.0004362c'^2 - 0.02752c' + 1.199$	0.679 to 1.255	B (1.85)
α_ϕ	$138.8\phi^{-1.366}$	0.861 to 1.485	B (1.72)
α_ξ	$3.414\xi^2 - 1.930\xi + 1.250$	0.908 to 1.218	C (1.34)
α_{K_0}	$-6.207K_0^2 + 6.807K_0 - 0.8492$	0.850 to 1.040	C (1.22)
α_D	$0.3865(D/h)^2 - 1.375(D/h) + 2.210$	0.978 to 1.147	C (1.17)

Table 5 - Influence factors for the maximum horizontal displacements of the wall.

Influence factor	Equation	Influence factor range	Impact grade
β_h	$0.02976h^{2.141}$	0.375 to 3.508	A (9.35)
β_ξ	$0.3193\xi^{-0.7131}$	0.651 to 2.137	A (3.28)
$\beta_{E_{50}}$	$10.80E_{50}^{-0.7009}$	0.544 to 1.761	A (3.24)
β_c	$0.0005111c'^2 - 0.03016c' + 1.218$	0.670 to 1.352	B (2.02)
β_{ρ_s}	$-0.1072 \ln(\rho_s) + 1.623$	0.752 to 1.379	B (1.83)
β_ϕ	$256.9\phi^{-1.535}$	0.880 to 1.495	B (1.70)
β_D	$-0.4153(D/h)^2 + 1.623(D/h) - 0.5279$	0.698 to 1.103	C (1.58)
β_{K_0}	$-7.666K_0^2 + 9.203K_0 - 1.683$	0.736 to 1.103	C (1.50)

of variable i on the maximum bending moment of the wall. Naturally, if one parameter is the same in the base and in the *target excavation*, it is not necessary to calculate the corresponding correction factor, as the influence factors are the same and thus their ratio is 1.

Table 4 contains a list of the equations that allow the calculation of the different influence factors for the bending moment, to be included in Eq. (6). These equations result from an extensive parametric study presented in the companion paper (Raposo *et al.*, 2017).

Considering the application of the method, it is crucial to know which parameters are more relevant, *i.e.*, those whose variation has greater consequences on the wall maximum bending moment.

The definition of the impact grade of each parameter was performed by analysing the range of the influence factor. This range, shown in the third column of Table 4, was defined from the extreme values of the parametric study done by Raposo *et al.* (2017) and not from the equation defining the influence factor. The ratio between the upper and lower limits of the range is presented inside brackets in the last column of Table 4. Taking this numerical classification as a starting point, a qualitative scale from A to C was defined, aiming to simplify the interpretation of the table,

with A corresponding to a relevant impact and C to a reduced impact. It should be noticed that the minimum theoretical value of this ratio is 1, corresponding to a variable with no influence on the wall maximum bending moment.

2.3. Prediction of the maximum horizontal displacements of the wall and the ground surface

The prediction of the maximum wall displacement is performed through a methodology similar to the one presented for the maximum wall bending moment, using the following expression:

$$\delta h_{wall} = \delta h_{wall}^{ref} \times cd_h \times cd_D \times cd_\xi \times cd_{\rho_s} \times cd_{E_{50}} \times cd_\phi \times cd_c \times cd_{K_0} \quad (7)$$

which consists of multiplying the horizontal displacement of the wall, obtained in the *reference excavation*, by the several correction factors corresponding to the different variables.

As for the bending moments, the correction factors are obtained dividing the influence factors for the *target excavation* by the respective factors for the *reference excavation*, as expressed by the following equation:

$$cd_i = \frac{\beta_i(\text{target excavation})}{\beta_i(\text{reference excavation})} \tag{8}$$

where *i* represents the generic parameter and β_i the displacement influence factor for parameter *i*.

Table 5 presents the equations of the displacement influence factors and information on the range of each influence factor. In the rightmost column of the table is presented a classification regarding the impact grade of each parameter, *i.e.*, its ability to influence the maximum horizontal displacement of the wall. Again, the impact grade of each parameter was determined by the range of the influence factor, similarly to the procedure adopted for the maximum wall bending moment.

In the parametric study described in the companion paper (Raposo *et al.*, 2017), a global analysis of the displacements was performed and it was clear the correlation between the maximum horizontal displacement of the wall and the maximum horizontal displacements of the surface. Having in mind the strong correlation between these two variables, the maximum horizontal displacement of the surface of the supported ground may be estimated by the following equation:

$$\delta h_{\text{surface}}^{\text{max}} = 0.54 \delta h_{\text{wall}}^{\text{max}} \tag{9}$$

2.4. Validation of the proposed method

Once the *reference excavation* is chosen, the use of the method is simple and can be easily implemented in a spreadsheet. With Eqs. (5) and (7), respectively, the maximum wall bending moment and maximum horizontal displacement of the wall can be easily predicted. Table 4 and Table 5 present all the necessary equations for determining the correction factors.

Before applying the method, it was necessary to validate it within the range of excavations used. For this purpose, an automatic procedure was implemented in a spreadsheet and, for all the 158 calculated excavations, a prediction of the results was performed using the proposed method. It should be mentioned that in this case the choice of the *reference excavation* was relatively evident as any calculation was defined varying just one parameter with respect to its *base excavation*. In such conditions the *reference excavation* was assumed to be the *base excavation*.

The accuracy of the method was evaluated through the calculation of a parameter named relative deviation, *Rd*, which consists on the deviation between the predicted and calculated results, as follows:

$$Rd = \frac{pv - cv}{cv} \tag{10}$$

where *pv* corresponds to the predicted value using the proposed method and *cv* to the calculated value using the finite element method.

Table 6 presents the maximum and minimum values of *Rd* obtained in the 158 calculations performed. Negative values mean that the predicted value is lower than the calculated value. Although certain values seem too large, they result from the reduced magnitude of the variables involved. This is the case of the calculation corresponding to the maximum *Rd*, in which the predicted value for the maximum wall displacement is 7.1 mm while the calculated value is 4.5 mm. The value of *Rd* is 60%, although the real difference is only 2.6 mm, which can be considered small for practical purposes.

Table 6 also presents the average of the obtained *Rd* for two different situations: the column defined as Absolute Average is obtained using the modulus of *Rd*; the column defined as Average is obtained using the real value of *Rd*, which may be positive or negative. The Absolute Average is necessarily bigger than the real average, where positive and negative *Rd* values tend to compensate each other. If the Average *Rd* was significantly different from zero, some incongruence in the method would have occurred.

Although the maximum *Rd* achieves relevant values, the Absolute Average is significantly lower, assuming the values of 4.2% for the maximum wall bending moment and 7.8% for the maximum horizontal displacement of the wall. These values certify the accuracy of the procedure presented in this paper. Additionally, the average of the *Rd* values is very close to zero, constituting a preliminary validation for the proposed methodology.

Finally, it must be referred that the accuracy in predicting bending moments is much higher than the accuracy in predicting displacements, either of the wall or of the ground. This result was expected, as the influence factors regarding the maximum horizontal displacements of the wall are bigger than the ones referring to the bending moments. The product of the eight values that measure the impact grade regarding the bending moments (Table 4) is 373.2, while the same product for the maximum horizontal displacements of the wall (Table 5) is 1479.9, proving the higher variability of the latter.

2.5. Alternative methodology for selection of the Reference Excavation

An alternative procedure to overcome the difficulty of choosing the *reference excavation* is based not in the selection of a single *reference excavation*, but in using all the four *base excavations* as starting points for the parametric study. These excavations were presented in Table 2 and are

Table 6 - Relative deviation between predicted and calculated values.

	Maximum	Minimum	Absolute average	Average
M_{max}	38.9%	-11.4%	4.2%	0.4%
δh_{wall}	60.0%	-22.3%	7.8%	0.5%

described in detail in the companion paper. Starting from the four base excavations, it is possible to make four different predictions. The average of those predictions should be close to the value obtained through calculations using the Finite Element Method.

This strategy presents two great advantages: it eliminates the difficulty of choosing the *reference excavation* and attenuates local disturbances in the functions expressing the maximum bending moment and horizontal displacement of the wall, resulting in very satisfactory predictions. The main disadvantage results from the attempt to approximate these functions from excavations amply different from the *target excavation*, transforming the method in a purely mathematical process, and thus totally neglecting the necessary engineering judgment for this type of problems.

3. Examples

3.1. Strategy for choosing the examples

Although the description of the method has been thoroughly explained in the previous sections, some examples are performed for its full understanding, with the additional advantage of contributing to the validation of the proposed methodology.

The selection of the examples follows a strategy of increasing difficulty in the choice of the *reference excavation*, allowing the reader to understand and master the proposed methodology.

Example 1 is intended to be as simple as possible. In such conditions, it shall be almost coincident with one of the *reference excavations*, varying just one parameter. The simplicity of the example should not create any difficulty in selecting the *reference excavation* and lead to satisfactory results.

Example 2 corresponds to an additional step in the difficulty of selecting the *reference excavation*, particularly focusing the doubt on two *reference excavations*. An example was created whose geometry is coincident with geometry 1, presented in the companion paper, but the geotechnical properties of the excavated soil are in between the properties adopted for geotechnical scenarios 1 and 2. In such conditions, the doubt in selecting the best *reference excavation* arises.

Example 3 intends to demonstrate the application to an excavation where both the geometrical conditions and the geotechnical scenario are significantly different from any of the *reference excavations*. This situation can lead to some difficulty in choosing the best *reference excavation* and so, taking advantage of the situation, alternative methodologies for selecting the reference excavation are discussed.

The purpose of Example 4 is to show an extra capability of the proposed method, which is the possibility of im-

proving itself by integrating results from new calculations or even real monitoring results.

All the predictions performed in the previous examples result from interpolations based in the several calculations performed. Naturally, extrapolating out of the calculated ranges might lead to results with reduced confidence or even to poor results. The purpose of Example 5 is to show the risk of applying the method to excavations clearly different from the ones previously used to define the influence functions and, particularly, the risk of predicting results for situations out of the validated range of each parameter.

Table 7 presents the values of the several parameters characterizing the excavations adopted as examples, as well as the parameters of the excavations #A00 to #D00, chosen as *reference excavations*.

3.2. Example 1

In the first, necessarily simple, example, the proposed preliminary design method will be used to estimate the maximum wall bending moment and maximum wall horizontal displacement for the excavation nominated #Ex1. As can be observed in Table 7 and Fig. 1, this excavation is identical to the *reference excavation* #A00, except for the parameter ρ_s (support system stiffness), justifying the choice of excavation #A00 as *reference excavation*. In such conditions, only the correction factor regarding the support system stiffness needs to be calculated, as all the other factors are equal to one.

Using the equations presented in Table 4, it is possible to determine the following values of factors α_{ρ_s} for the *target excavation* (#Ex1) and for the *reference excavation* (#A00), respectively:

$$\alpha_{\rho_s, =180} = 0.04424 \times 180^{0.5318} = 0.700 \quad (11)$$

and

$$\alpha_{\rho_s, =100} = 0.04424 \times 100^{0.5318} = 0.512 \quad (12)$$

Table 7 - Main characteristics of the excavations used in the examples.

Excavation	h (m)	ρ_s	ξ	D/h	E_{s0} (MPa)	ϕ' (°)	c' (kPa)	K_0
#A00	15	100	0.15	1.6	22.5	33	12	0.40
#B00	15	100	0.15	1.6	37.5	37	21	0.60
#C00	25	350	0.20	1.2	22.5	33	10	0.40
#D00	25	350	0.20	1.2	37.5	37	20	0.60
#Ex1	15	180	0.15	1.6	22.5	33	12	0.40
#Ex2	15	100	0.15	1.6	30.0	35	16.5	0.50
#Ex3	17.5	250	0.17	1.25	30.0	35	15	0.55
#Ex4	17.5	250	0.24	1.25	30.0	35	15	0.55
#Ex5	30	700	0.15	1.4	70.0	40	40	0.50

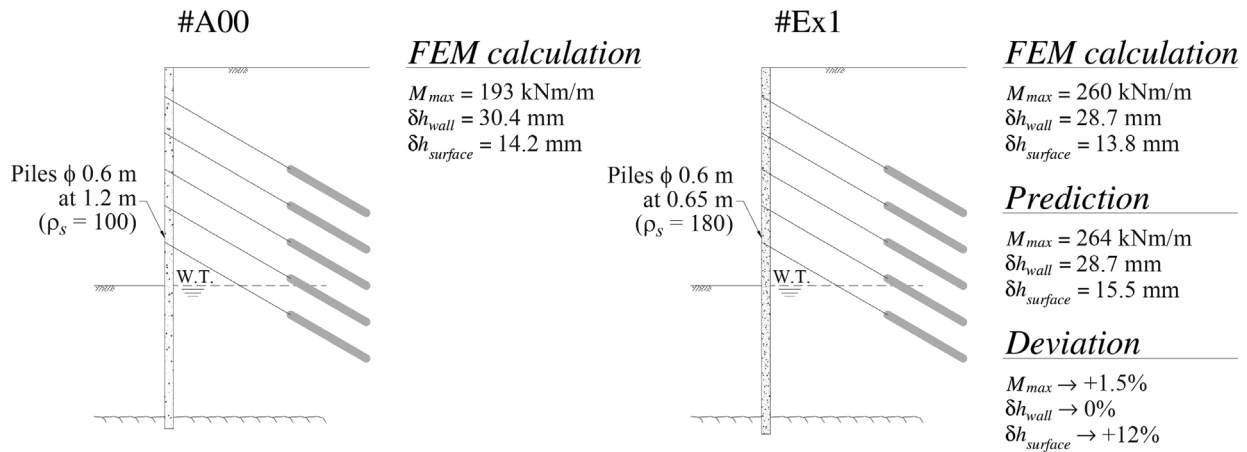


Figure 1 - Example 1: Excavation characteristics and results.

The ratio of these two values results in the correction factor for the maximum bending moment, cm_{ps} , of 1.367. Considering the maximum bending moment obtained in calculation #A00 (193 kNm/m, as shown in Fig. 1) and using Eq. (5), the estimated bending moment for excavation #Ex1 is 264 kNm/m.

Adopting the same procedure for the maximum horizontal displacement of the wall, the coefficients β_{ps} for both excavations are obtained using the equation presented in Table 5:

$$\beta_{p_s=180} = -0.1072 \ln(180) + 1.623 = 1.066 \quad (13)$$

and

$$\beta_{p_s=100} = -0.1072 \ln(100) + 1.623 = 1.129 \quad (14)$$

The ratio of these two values corresponds to the correction factor regarding the maximum horizontal displacement of the wall, whose value is 0.944. Using Eq. (7), a horizontal displacement for excavation #Ex1 of 28.7 mm is obtained, which is roughly 5.6% lower than the one corresponding to excavation #A00.

The predicted maximum horizontal displacements at the surface, obtained using Eq. (9), is equal to 15.5 mm.

Figure 1 presents a summary of the predicted and calculated values. The relative difference, Rd , is lower than 2% in the case of the bending moments. Curiously, for the horizontal displacements of the wall, the prediction coincides with the calculations. Regarding the horizontal displacements of the surface, the difference between the prediction and the calculation is 12% of the latter. This difference is typically higher than the differences in the bending moments and the horizontal displacement of the wall, as a second order estimation is used.

3.3. Example 2

In the previous example, the selection of the *reference excavation* was obvious as excavation #A00 was totally coincident with Example 1, except for the support

system stiffness. In Example 2, as can be seen in Fig. 2, the geometric conditions are coincident with the *reference excavations* #A00 and #B00, while the geotechnical properties, namely E_{s0} , ϕ' , c' and K_0 , are exactly the mean values of the geotechnical properties of the two *reference excavations* (#A00 and #B00).

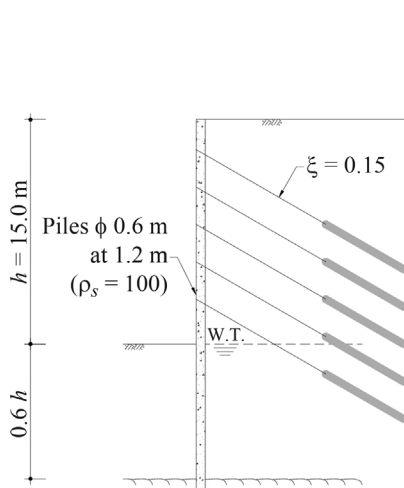
In such conditions, both excavations, #A00 and #B00, could be properly adopted as *reference excavations*. Figure 2 illustrates the results obtained for Example 2 adopting as *reference excavation* either excavation #A00 or excavation #B00.

Similarly to what was done in example 1, the equations presented in Table 4 were used to calculate the influence factors α_s , while the equations presented in Table 5 were used to calculate the factors β_s . Table 8 presents all influence and correction factors for Example 2, excavation #A00 and excavation #B00. The last column of the table shows the product of the several correction factors and, thus, it is an indirect measure of the difference between the chosen *reference excavation* and Example 3.

The predictions obtained are, in any situation, quite satisfactory, reaching a maximum Rd of 6.9% in the case of the maximum horizontal wall displacement. Regarding the bending moments, the deviations are both below 2.4%, which may be considered as an excellent result for preliminary design purposes.

Although *reference excavations* #A00 and #B00 could, apparently, be equally adopted, from the results presented in Fig. 2 it is clear that the quality of the prediction is dependent on the chosen *reference excavation*. Particularly for example 2, excavation #A00 is a better reference for predicting the maximum horizontal displacements of the wall, while excavation #B00 is preferable for predicting the maximum wall bending moments. The justification for this apparent contradiction is related to the impact grade of each parameter, as seen in Table 4 and Table 5.

Having in mind the previous results, it is clear that the *reference excavation* should be as similar as possible to the



Soil properties

#A00	#Ex2	#B00
$E_{50} = 22.5$ MPa	$E_{50} = 30.0$ MPa	$E_{50} = 37.5$ MPa
$\phi' = 33^\circ$	$\phi' = 35^\circ$	$\phi' = 37^\circ$
$c' = 12$ kPa	$c' = 16.5$ kPa	$c' = 21$ kPa
$K_0 = 0.40$	$K_0 = 0.50$	$K_0 = 0.60$

FEM calculation

#A00	#Ex2	#B00
$M_{max} = 193$ kNm/m	$M_{max} = 167$ kNm/m	$M_{max} = 132$ kNm/m
$\delta h_{wall} = 30.4$ mm	$\delta h_{wall} = 26.1$ mm	$\delta h_{wall} = 19.4$ mm
$\delta h_{surface} = 14.2$ mm	$\delta h_{surface} = 12.7$ mm	$\delta h_{surface} = 9.9$ mm

Predictions of Ex2 results

Based on #A00	Based on #B00
$M_{max} = 163$ kNm/m (-2.4%)	$M_{max} = 169$ kNm/m (+1.2%)
$\delta h_{wall} = 27.3$ mm (+4.6%)	$\delta h_{wall} = 24.3$ mm (-6.9%)
$\delta h_{surface} = 14.7$ mm (+15.7%)	$\delta h_{surface} = 13.1$ mm (+31%)

Figure 2 - Example 2: Excavation characteristics and results.

Table 8 - Example 2: influence factors and correction factors.

	h	ρ_s	ξ	D/h	E_{50}	ϕ'	c'	K_0	Product
α_i (#Ex2)	0.987	0.512	1.037	0.998	0.995	1.079	0.863	1.003	-
α_i (#A00)	0.987	0.512	1.037	0.998	1.143	1.170	0.931	0.880	-
cm_i (#A00)	1.000	1.000	1.000	1.000	0.871	0.923	0.927	1.139	0.849
α_i (#B00)	0.987	0.512	1.037	0.998	0.894	1.001	0.812	1.000	-
cm_i (#B00)	1.000	1.000	1.000	1.000	1.113	1.079	1.062	1.002	1.278
β_i (#Ex2)	0.981	1.129	1.235	1.006	0.996	1.096	0.860	1.002	-
β_i (#A00)	0.981	1.129	1.235	1.006	1.218	1.199	0.930	0.772	-
cd_i (#A00)	1.000	1.000	1.000	1.000	0.817	0.914	0.925	1.299	0.897
β_i (#B00)	0.981	1.129	1.235	1.006	0.852	1.006	0.810	1.079	-
cd_i (#B00)	1.000	1.000	1.000	1.000	1.169	1.089	1.061	0.929	1.255

target excavation, favouring the parameters with higher impact grade. This observation confirms the difficulty in choosing the best reference excavation, given the fact that the concept of “as similar as possible” may not be evident.

3.4. Example 3

In the third example, the target excavation is designated #Ex3, whose characteristics are presented in Table 7 and illustrated in Fig. 3. In this case, the choice of the reference excavation is not immediate as all the parameters differ from those of all of the four Base Excavations and, thus, any of them could be used as reference. Table 9 presents the influence factors and correction factors for example 3.

Considering the results presented in Fig. 3, it is not clear which is the best reference excavation. For the maximum wall bending moments, the best reference would be excavation #D00, but excavations #A00 and #C00 can also conduce to very satisfactory predictions, with Rd values lower than 1.5%. Excavation #B00 leads to a higher Rd , and can be considered the worst reference excavation for predicting bending moments in example 4.

Concerning the maximum wall horizontal displacements, excavations #A00 and #D00 give very satisfactory results. On the other hand, the predictions based on excavations #B00 and #C00 are quite different from the results obtained with the numerical calculations.

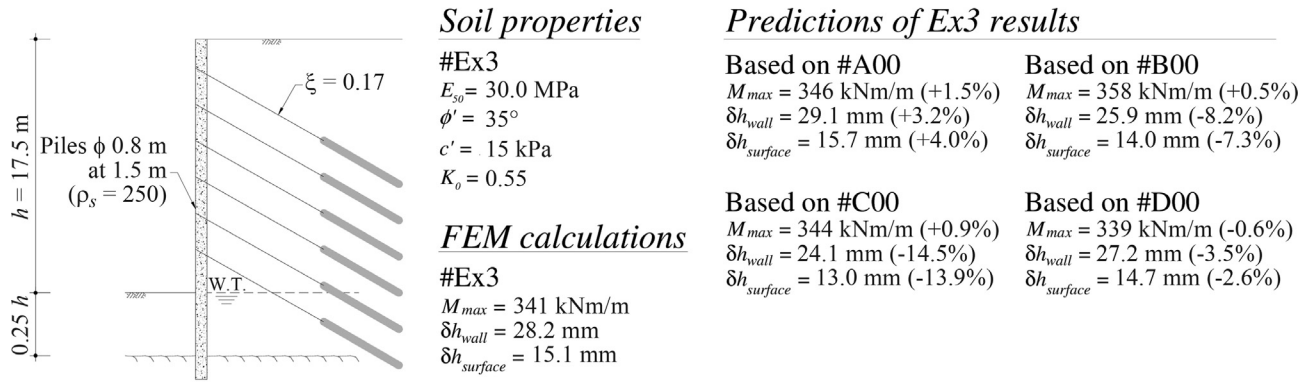


Figure 3 - Example 3: Excavation characteristics and results.

Table 9 - Example 3: influence factors and correction factors.

	h	ρ_s	ξ	D/h	E_{50}	ϕ'	c'	K_0	Product
α_i (#Ex3)	1.146	0.834	1.021	1.094	0.995	1.079	0.883	1.017	-
α_i (#A00)	0.987	0.512	1.037	0.998	1.143	1.170	0.931	0.880	-
cm_i (#A00)	1.162	1.628	0.984	1.096	0.871	0.923	0.949	1.155	1.797
α_i (#B00)	0.987	0.512	1.037	0.998	0.894	1.001	0.812	1.000	-
cm_i (#B00)	1.162	1.628	0.984	1.096	1.113	1.079	1.088	1.017	2.709
α_i (#C00)	1.621	0.997	1.001	1.115	1.143	1.170	0.967	0.880	-
cm_i (#C00)	0.707	0.836	1.020	0.981	0.871	0.923	0.914	1.155	0.501
α_i (#D00)	1.621	0.997	1.001	1.115	0.894	1.001	0.822	1.000	-
cm_i (#D00)	0.707	0.836	1.020	0.981	1.113	1.079	1.075	1.017	0.776
β_i (#Ex3)	1.365	1.031	1.130	0.852	0.996	1.096	0.881	1.060	-
β_i (#A00)	0.981	1.129	1.235	1.006	1.218	1.199	0.930	0.772	-
cd_i (#A00)	1.391	0.913	0.915	0.847	0.817	0.914	0.947	1.373	0.956
β_i (#B00)	0.981	1.129	1.235	1.006	0.852	1.006	0.810	1.079	-
cd_i (#B00)	1.391	0.913	0.915	0.847	1.169	1.089	1.087	0.982	1.338
β_i (#C00)	2.928	0.995	1.006	0.822	1.218	1.199	0.968	0.772	-
cd_i (#C00)	0.466	1.036	1.123	1.037	0.817	0.914	0.910	1.373	0.525
β_i (#D00)	2.928	0.995	1.006	0.822	0.852	1.006	0.819	1.079	-
cd_i (#D00)	0.466	1.036	1.123	1.037	1.169	1.089	1.075	0.982	0.756

In any case, the predicted values are very satisfactory having in mind that the proposed method aims to be used for preliminary design purposes. Independently of the reference excavation, the maximum Rd is 5.0% for the maximum bending moment, and 14.5% for the maximum horizontal wall displacements. These values are totally acceptable for preliminary design.

Despite the overall good results of the predictions, the method could be improved if the choice of the reference excavation was the most adequate, as it plays a vital role in the predictions.

As can be observed from the values in Fig. 3, the estimated values are close to the values obtained using the Finite Element Method, with the maximum difference around 8%. As the relative errors are negative, this means that the estimated values are lower than those obtained by the finite element calculations.

Example 3 is a typical case in which the predictions may be performed in a totally automatic mode, i.e., without the need for choosing a reference excavation, as explained in section 2.5.

Considering the results obtained using the Finite Element Method as correct, the maximum error resulting from

the use of the proposed method, presented in brackets in Table 10, is lower than 10% for both bending moment and displacement. Apparently, using the automatic procedure, based on the use of the four *reference excavations* simultaneously, it is possible to have results with similar or better accuracy than using a single *reference excavation*.

3.5. Example 4

The main purpose of the fourth example is to illustrate another capability of the proposed method: the possibility to progress by integrating new results (or monitoring data from real construction sites).

Suppose that the actual bending moments and displacements of excavation #Ex3 are known. Admit now that it is important to evaluate the effect of increasing the anchor prestressing, which would result in a different excavation, nominated from now on #Ex4. Admit that the prestress will be increased from 167 kN/m to 233 kN/m. This increase corresponds to a variation in the prestressing index from 0.17 to 0.24, as shown in Fig. 4.

Using the method presented in this paper, it is only necessary to determine the correction factors corresponding to the prestressing index (cm_ξ and cd_ξ) and to multiply

each of them by the bending moments and horizontal displacements of the wall for excavation #Ex3, respectively.

Table 11 presents the influence factors and correction factors for the problem. Bearing in mind the values for the correction factors cm_ξ and cd_ξ , the increase in prestress from 167 kN/m to 233 kN/m, maintaining all the other characteristics of the excavation, will produce a reduction of the bending moment of around 4% (cm_ξ is equal to 0.964) and a reduction of the maximum horizontal displacement of the wall close to 20% (cd_ξ is equal to 0.782).

Both, the predicted values and the values obtained with the Finite Element Method, were included in Fig. 4, together with the difference between them. As can be observed, the deviations obtained are minimal.

This example proves that the accuracy of the methodology used in the predictions can improve itself by incorporating new data, creating a kind of Bayesian knowledge.

3.6. Example 5

The final example intends to illustrate the risk of using the proposed methodology in conditions significantly different from the ones validated with the several calculations performed. The excavation in this example has 3 parameters outside the studied range. Fig. 5 presents the geotechnical and geometric characteristics of #Ex5. The excavation depth increased to 30 m, 5 m more than the maximum excavation tested, the cohesion of the ground is assumed to be 40 kPa, while the assumed validation range for this parameter had a maximum of 30 kPa, and the soil stiffness is characterized by an E_{50} of 70 MPa, a value also

Table 10 - Example 3: Estimated and calculated values.

Reference excavation	M_{max} (kNm/m)	δh_{wall} (mm)	$\delta h_{surface}$ (mm)
#A00	346 (+1.5%)	29.1 (+3.2%)	15.7 (+4.0%)
#B00	358 (5.0%)	25.9 (-8.2%)	14.0 (-7.3%)
#C00	344 (+0.9%)	24.1 (-14.5%)	13.0 (-13.9%)
#D00	339 (-0.6%)	27.2 (-3.5%)	14.7 (-2.6%)
Average	347 (1.8%)	26.6 (-5.7%)	14.4 (-4.6%)
FEM	341	28.2	15.1

Table 11 - Example 4: influence factors and correction factors.

α_ξ (#Ex4)	0.983	β_ξ (#Ex4)	0.883
α_ξ (#Ex3)	1.021	β_ξ (#Ex3)	1.130
cm_ξ (#Ex4, #Ex3)	0.964	cd_ξ (#Ex4, #Ex3)	0.782

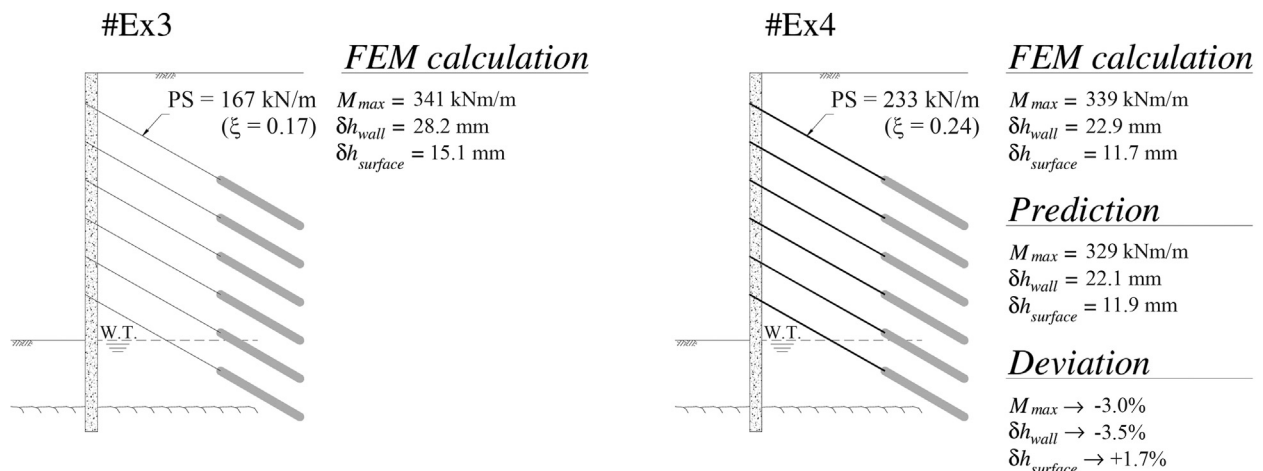


Figure 4 - Example 4: Excavation characteristics and results.

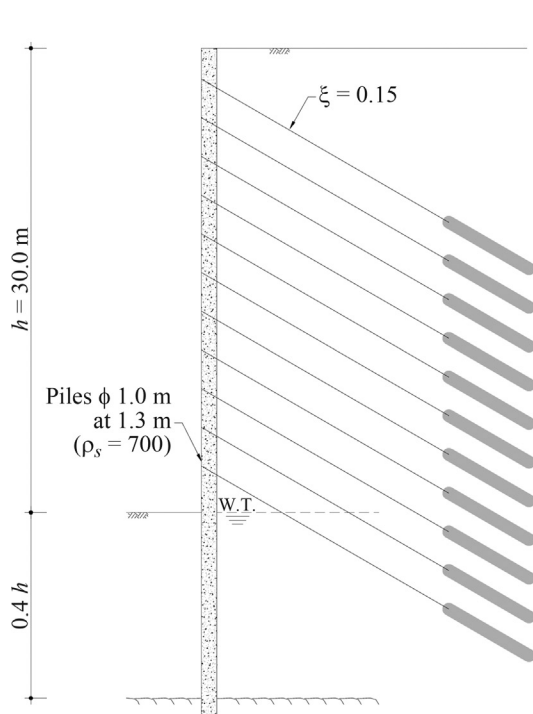


Figure 5 - Example 5: Excavation characteristics and results.

higher than the maximum Young modulus previously used. All the remaining parameters were within the validation ranges used.

Although the parameters out of the validation range were not significantly outside the range, the results presented in Fig. 5 clearly show that the obtained R_d are markedly higher than the equivalent deviations in the previous examples. In this case these R_d values are always above 10% and, in most of the situations, above 20%. Extreme values of 40% are obtained.

The example presented proves that the proposed methodology has to be used with caution and extrapolations should be avoided. In any case, preliminary design information may be obtained and the evolutionary characteristic of the method allows future developments in order to enlarge the range of geotechnical and geometrical scenarios.

4. Final Considerations

This paper proves the utility of a novel procedure that may be used for the preliminary design of earth retaining structures. Although the calculations performed for validation have indicated that this method is capable of predicting the maximum bending moment and maximum wall displacements with appreciable accuracy, it is imperative to emphasize that, in particular situations, relevant discrepancies may occur between the estimated values and those calculated through the Finite Element Method.

A particular example of what was referred in the previous paragraph is related to the support system stiffness. Although in its conceptual definition the distance between

Soil properties

#Ex5
 $E_{s0} = 70 \text{ MPa}$
 $\phi' = 40^\circ$
 $c' = 40 \text{ kPa}$
 $K_0 = 0.50$

FEM calculations

#Ex5
 $M_{max} = 390 \text{ kNm/m}$
 $\delta h_{wall} = 29.8 \text{ mm}$
 $\delta h_{surface} = 15.2 \text{ mm}$

Predictions of Ex5 results

Based on #A00
 $M_{max} = 480 \text{ kNm/m (+23\%)}$
 $\delta h_{wall} = 39.4 \text{ mm (+32\%)}$
 $\delta h_{surface} = 21.3 \text{ mm (+40\%)}$

Based on #C00
 $M_{max} = 476 \text{ kNm/m (+22\%)}$
 $\delta h_{wall} = 32.7 \text{ mm (+10\%)}$
 $\delta h_{surface} = 17.7 \text{ mm (+16\%)}$

Based on #B00
 $M_{max} = 497 \text{ kNm/m (+27\%)}$
 $\delta h_{wall} = 35.1 \text{ mm (+18\%)}$
 $\delta h_{surface} = 18.9 \text{ mm (+25\%)}$

Based on #D00
 $M_{max} = 470 \text{ kNm/m (+21\%)}$
 $\delta h_{wall} = 36.8 \text{ mm (+23\%)}$
 $\delta h_{surface} = 19.9 \text{ mm (+31\%)}$

anchors is included, the numerous tests performed proved that, in certain cases, this parameter is not enough to guarantee the quality of the estimation. The conclusion to be extracted from the results is that the critical spacing is the one referring to the distance between the last level of anchors and the bottom of the excavation. It was also noticed that, when the critical spacing differs from the value of 3.0 m, the value adopted for all the excavations, the estimated values may significantly diverge from the calculated ones.

Despite this handicap, the method presents its own utility. It is only necessary to consider another correction factor that takes the above mentioned aspects into consideration. One of the great advantages of the proposed method is its ability to evolve, being possible to include or exclude parameters at any moment in order to take into account any particular aspect.

The vital phase in the application of the proposed methodology is the definition of the geometrical parameters of the excavation and respective ground properties. The consecutive use of the method will increment its accuracy and confidence. Even having in mind that access to finite element codes is nowadays easy, the method may be used for an additional and different check.

The illustrated examples contribute for clarifying how to use the procedure, but also demonstrate the good results and accuracy of the methodology.

In spite of the global quality of the results, not only in the presented examples but also in many other calculations performed, it is important to refer that the method can make predictions by extrapolating from previous results, being

possible that important differences may occur in particular situations. Anyhow, these errors may be modest when compared to the difficulty in accurately defining parameters such as stiffness or the initial stress state of the ground, making the method appropriate for preliminary design purposes.

5. Appendix A –Mathematical Formulation of the Proposed Method

In order to clarify the *modus faciendi* of the proposed method for estimating forces and displacements, this section is devoted to its detailing and explanation.

From a mathematical point of view, this problem consists in determining the value of an unknown function, knowing the values of the variables the function depends on. In order to explain the adopted procedure, the function $Z(x, y)$, will be used as an example. This function, represented in Fig. 6, has the following analytical equation:

$$Z(x, y) = (x^2 - 2x + 3)(\log(y - 9) + 0.3) + 0.2x + 4 \quad (15)$$

The starting step consists in the definition of two points, from now on designated as “base points”. The choice of these points did not follow any specific rule but they should be located as much apart as possible within the studied domain.

Figure 7 shows the base points used in this example. The adopted points, in this case, correspond to the squares identified by 1 and 2, and have the following coordinates:

- Base point 1: $(x = 1, y = 2)$;
- Base point 2: $(x = 2.5, h = 16)$.

Picking each of the base points, the function was computed assuming for x all the possible values in the range $\{0, 0.5, 1, 1.5, 2, 2.5, 3\}$, resulting in the points shown in Fig. 7. Using the method of least squares, these points can be approximated by two curves that reflect the influence of parameter x . For function $Z(x, y)$, defined by Eq. (15), the

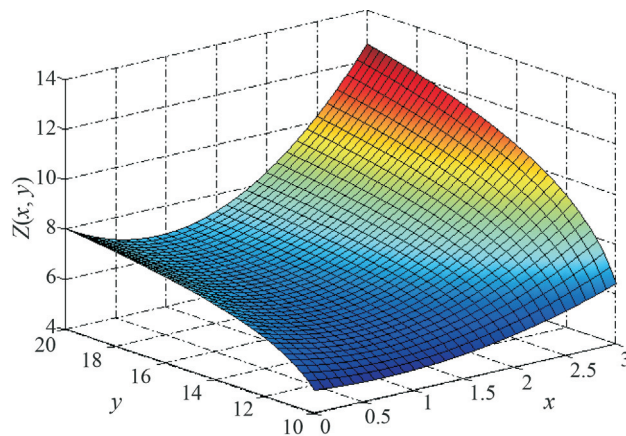


Figure 6 - Three-dimensional representation of the function $Z(x, y)$.

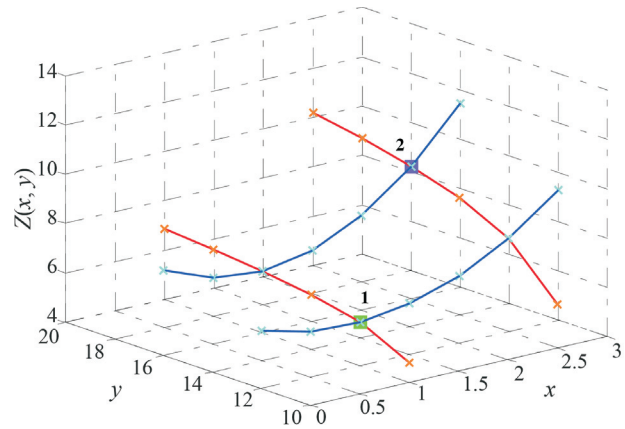


Figure 7 - Base points and one-dimensional analysis.

curves represented in Fig. 7 by the lines with constant y correspond to:

$$f_{y=12}(x) = 0.7771x^2 - 1.354x + 6.331 \quad (16)$$

and

$$f_{y=16}(x) = 1.145x^2 - 2.090x + 7.435 \quad (17)$$

These curves can be placed in the same vertical plane, as shown in Fig. 8a, and then n with respect to any point in the domain. Setting $x = 1.5$ as the normalization reference value, as shown in Fig. 8b, it is possible to determine an average normalized influence curve for variable x , in this case defined by the following equation:

$$f_{med}(x) = 0.1450x^2 - 0.2639x + 1.064 \quad (18)$$

Adopting the same method for variable y , the following equation is obtained:

$$g_{med}(y) = 0.5763 \log(y - 9) + 1 \quad (19)$$

After determining the average influence curves for each variable, it is possible to estimate the value of $Z(x, y)$ in any point of the domain. It is, of course, possible to estimate values of $Z(x, y)$ using values of x or y out of their domain of variation, but that procedure should be avoided as it can produce significant errors.

In order to calculate $Z'(x, y)$, the function that represents the estimated value for $Z(x, y)$ in any point with coordinates (x, y) , a scalar α should be multiplied by both functions of the average influence of each of the variables, $f_{med}(x)$ and $g_{med}(y)$, as defined by the following equation:

$$Z'(x, y) = \alpha f_{med}(x) g_{med}(y) \quad (20)$$

Factor α is determined from a known point of the function $Z(x, y)$ in such a way that $Z'(x, y)$ matches $Z(x, y)$ in that point. Eq. (20) may be rewritten as:

$$Z'(x, y) = Z(a, b)c(x)c(y) \quad (21)$$

where $c(y)$ is equal to $f_{med}(x)/f_{med}(a)$ and $c(x)$ corresponds to $g_{med}(y)/g_{med}(b)$.

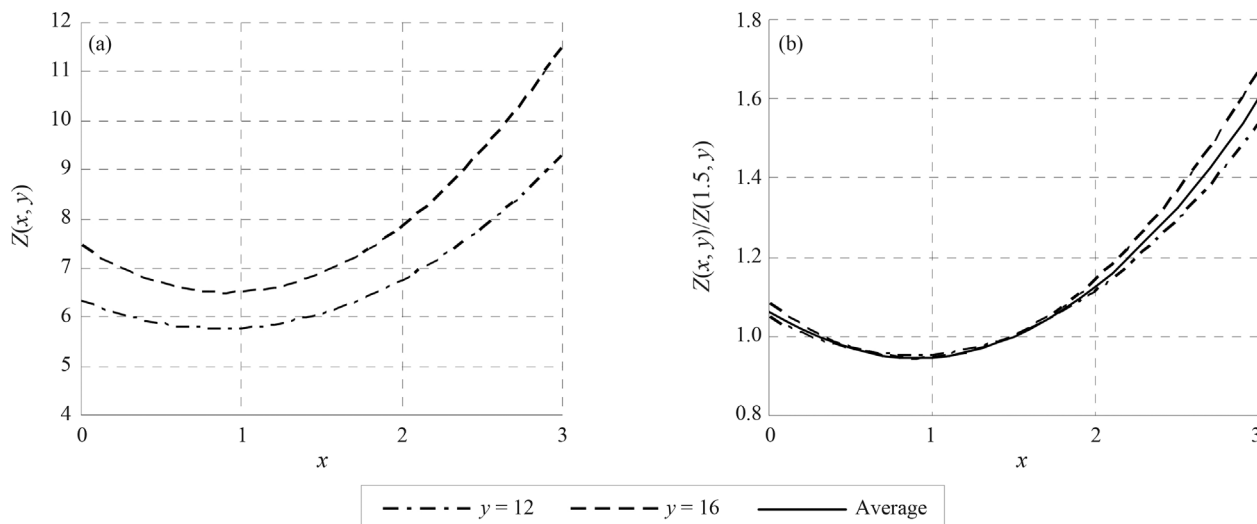


Figure 8 - Parametric analysis for variable x .

Equation (21) clarifies the procedure adopted in the proposed preliminary design method and shows how, starting from a known value of the function $Z(a, b)$, the value for the function in another point can be estimated, by multiplying it by the corrective factors $c(x)$ and $c(y)$, each corresponding to a variable in the function.

Figure 9 shows the overlapping of the function $Z(x, y)$, defined by the opaque surface, and the function $Z'(x, y)$, defined by the grid. To define the function $Z'(x, y)$ the two functions were forced to coincide at point (2.5,16), corresponding to base point 2, and shown in Fig. 9 by a square. The parameter α assumed, in this case, the value 4.75. In certain areas of Fig. 9 the grid representing the function $Z'(x, y)$ is not visible as it is below the surface representing the function $Z(x, y)$.

Raposo (2007) presents a detailed description of the methodology briefly presented in the preceding paragraphs. A similar procedure was adopted for the functions maximum bending moment and maximum horizontal dis-

placement of the wall. For this purpose, individual analysis of each variable were performed starting from 4 different *base excavations*.

Acknowledgments

This work was financially supported by: Project POCI-01-0145-FEDER-007457 – CONSTRUCT - Institute of R&D in Structures and Construction funded by FEDER funds through COMPETE2020 - Programa Operacional Competitividade e Internacionalização (POCI) – and by national funds through FCT - Fundação para a Ciência e a Tecnologia.

References

- Mana, A.I. (1978). Finite Element Analyses of Deep Excavation Behavior in Soft Clay. PhD Thesis, Stanford University.
- Mana, A.I. & Clough, G.W. (1981). Prediction of movements for braced cuts in clay. *Journal of Geotechnical and Geoenvironmental Engineering* 107(GT6), p. 759-777.
- Raposo, N.P. (2007). Pré-Dimensionamento de Estruturas de Contenção Ancoradas. MSc Thesis, Universidade do Porto.
- Raposo, N.P.; Topa Gomes, A. & Matos Fernandes, M. (2017). Anchored Retaining Walls in Granite Residual Soils; I - Parametric Study. *Soils and Rocks* 40(3):229-242.

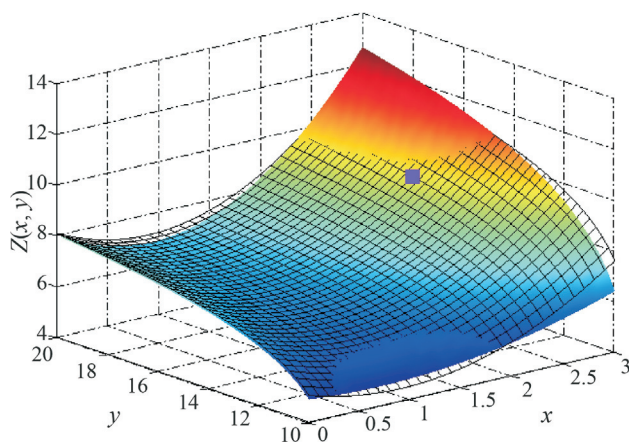


Figure 9 - Function $Z'(x, y)$, function $Z(x, y)$ and base point 2.